Performance of Reinforced Concrete Beams Strengthened in Shear Using L-Shaped CFRP Plates - An Experimental Investigation

Amir Mofidi[1], Sébastien Thivierge[2], Omar Chaallal[3], and Yixin Shao[4]

Abstract

This paper presents results of an experimental investigation on reinforced concrete (RC) T-beams retrofitted in shear with prefabricated L-shaped carbon fibre-reinforced polymer (CFRP) plates. Shear-strengthening of RC beams with L-shaped fibre-reinforced polymer (FRP) plates has proved effective. In this method, grooves are made throughout the beam flange to embed fully the vertical leg (perpendicular to the longitudinal axis of the RC beam and in the RC beam web surface) of the L-shaped CFRP plate. However, in some cases, drilling grooves in the concrete flange might not be feasible because of the presence of obstacles such as longitudinal steel in the flange of the RC beams. Therefore, the main objective of this investigation was to evaluate the performance of the RC beams strengthened in shear with externally bonded L-shaped as affected by the embedment length of the L-shaped FRP plates.

[1] Postdoctoral Fellow, Department of Civil Engineering and Applied Mechanics, McGill University, 817 Sherbrooke West, Montreal QC Canada H3A 0C3. E-mail: amir.mofidi@mail.mcgill.ca.

[2] Master of Science Graduate, University of Quebec, École de Technologie Supérieure, 1100 Notre-Dame West, Montreal QC Canada H3C 1K3.

[3] Professor of Construction Engineering, University of Quebec, École de Technologie Supérieure, 1100 Notre-Dame West, Montreal QC Canada H3C 1K3 (corresponding author). E-mail: omar.chaallal@etsmtl.ca.

[4] Associate Professor, Department of Civil Engineering and Applied Science, McGill University, Sherbrooke West, Quebec, Canada H3A 0C3. E-mail: yixin.shao@mcgill.ca.

In total, six tests were performed on 2500 mm-long T-beams. Three specimens were strengthened in shear using epoxy-bonded L-shaped CFRP plates with different embedment lengths in the RC beam flange. One specimen was shear-strengthened with fully embedded CFRP plates in the concrete beam flange. The second specimen was strengthened with partial embedment of the L-shaped CFRP plate. This specimen is representative of the case where full penetration of the CFRP plate is not feasible because of an obstacle. In this specimen, the embedment length was set to 25 mm to simulate the minimum concrete cover thickness in RC beams. The third specimen was shear-strengthened with L-shaped CFRP plates with no embedment in the concrete beam flange. In addition, the performance of the beams strengthened with L-shaped CFRP plates was compared with that of a similar specimen strengthened with externally bonded (EB) FRP sheets without embedment. Results show that the performance of the specimens strengthened with partially and fully embedded L-shaped CFRP plates in the beam flange was superior to that of the beams strengthened with EB FRP sheets and L-shaped CFRP plates with no embedment.

CE Database subject headings: Concrete beam; Fibre-reinforced polymer; Strengthening; Shear; Epoxy bonding; Debonding; Embedment; L-shaped plates.

INTRODUCTION

In the last two decades, the application of fibre-reinforced polymer (FRP) composites has received much attention in the construction engineering industry, particularly for rehabilitation of reinforced concrete (RC) structures. Consequently, many valuable research studies on different aspects of the subject, including shear-strengthening of RC beams with FRP composites, have been conducted (e.g., Uji 1992; Chaallal *et al.* 1998; Khalifa *et al.* 1998; Triantafillou 1998; Czaderski 1998; Chen and Teng 2003; De Lorenzis 2004; and Mofidi and Chaallal 2011a,b). Different techniques such as externally bonded (EB) FRP sheets, near-surface mounted (NSM) FRP rods, and embedded through-section (ETS) FRP rods have been proposed and successfully tested for strengthening of RC beams and girders in shear with FRP composites (e.g., Uji 1992; Chaallal *et al.* 1998; De Lorenzis and Nanni 2001; Monti and Liotta 2006; De Lorenzis 2004; and Mofidi *et al.* 2012a,b).

Prefabricated L-shaped FRP plates present a potential alternative to EB FRP sheets, NSM FRP rods, and ETS FRP rods for shear strengthening of reinforced-concrete (RC) beams. Meier (1998) conducted a series of pull-out tests on L-shaped carbon-FRP (CFRP) plates bonded to concrete blocks. In addition, a series of tests on adhesively post-installed embedded (APE) CFRP plates bonded to concrete blocks was also carried out by Meier (1998). Czaderski (1998) investigated the effectiveness of L-shaped CFRP plates in shear-strengthening of RC beams. The test matrix of his investigation included three RC beams with different concrete cross-sectional properties and loading configurations. In 2002, an experimental investigation was conducted at the EMPA laboratories (Eidgenössische Materialprüfungs und Forschungsanstalt) on retrofitting RC beams with L-shaped CFRP plates, which can be described as follows: (i) two shear-strengthened specimens using L-shaped CFRP plates with different internal transverse-steel ratio were tested under static load; (ii) one test was implemented on a cracked RC beam strengthened under load in shear using L-shaped FRP plates; and finally (iii) one strengthened specimen was tested under cyclic loads. The results of this experimental investigation were published in EMPA Report No. 116/7 (2002). Later, Czaderski and Motavalli (2004) focused on the fatigue behavior of RC beams strengthened with L-shaped CFRP plates using the results of the EMPA tests

(2002). Chen and Robertson (2004) tested a pre-cracked, pre-stressed concrete T-beam retrofitted in shear using L-shaped CFRP plates. Later, Robertson *et al.* (2007) conducted a cyclic loading test on an AASHTO-type RC beam strengthened with L-shaped CFRP plates.

Clearly, very few tests have been performed worldwide on RC beams strengthened in shear with L-shaped FRP plates, and the need for more related data has been clearly demonstrated. Of all the tests implemented on retrofitted RC beams with L-shaped plates, few were performed under static load, and none considered partial embedment of RC beams in the flange because of an obstacle that inhibits full penetration. The main objective of this study is twofold: (1) to assess the effectiveness of shear-strengthening using bonded L-shaped CFRP plates with partial and full embedment compared to conventional EB FRP sheets, and (2) to evaluate the effect of embedment length into the flange on the performance of RC beams strengthened in shear with L-shaped laminates.

In a companion paper (Mofidi *et al.* 2013), design equations for RC beams strengthened with L-shaped CFRP plates were proposed. These equations were derived considering various observed failure modes, including FRP pull-out, concrete break-out in the flange, FRP plate debonding, and FRP overlap failure at the beam soffit. The proposed design equations showed reasonable correlation with experimental results.

EXPERIMENTAL INVESTIGATIONS

The RC beams were tested in three-point load flexure. Overall, the experimental program (Table 1) involved six tests performed on half-scale RC T-beams. The control specimen, which was not strengthened with carbon FRP (CFRP), was labelled CON, whereas the specimens retrofitted with L-shaped CFRP plates were labelled LS. The single specimen strengthened with a layer of EB CFRP sheet was labelled EB. In the specimens strengthened with L-shaped CFRP plates, the depth of plate embedment into the RC beam flange was indicated as follows: the beam strengthened with CFRP L-shaped plates with no embedment was labelled NE; the specimen strengthened with CFRP L-shaped plates partially embedded (25 mm) into the RC beam flange was labelled PE; and the beam strengthened with CFRP L-shaped plates fully embedded (102 mm) into the beam flange was labelled FE.

All the beams tested in this study were labelled S1, except for the S0-CON beam which had no transverse shear reinforcement (hereafter called transverse-steel). Series S1 corresponds to specimens with internal transverse-steel stirrups spaced at $s = d/2$, where $d = 350$ mm and represents the effective depth of the beam cross section (Fig. 1). Thus, for example, specimen S1-LS-PE features the beam with internal steel stirrups spaced at $s = d/2$, which was retrofitted with L-shaped plates embedded one inch into the RC beam flange. The labels used for each beam are provided in Table 1.

Specimens

The cross sections of the specimens and their dimensions are presented in Fig. 1. The tested specimens consisted of a T-beam with a web width of 152 mm and a flange depth of 102 mm. The RC beams had an overall length of 2500 mm and a span of 2100 mm. The load was applied at mid-span of the RC beam. The longitudinal-steel reinforcement at the bottom of the RC beam was laid in two layers of four 25M bars (diameter 25.2 mm, area 500 mm^2). At the top of the cross section, the longitudinal-steel reinforcement consisted of six 10M bars laid in one layer (diameter 10.3 mm, area 100 mm^2). The transverse-steel reinforcement was 8 mm in diameter (area 50 mm^2). The spacing between the steel stirrups was 175 mm ($d/2$) for all the specimens with internal transverse steel (Fig. 1). The specimens had chamfered outer corners at the sides of the beam soffit to match the curved corner shape of the CFRP L-shaped plates. The strengthening L-shaped FRP plates were epoxy-bonded mid-way between the steel stirrup locations.

Materials

The internal longitudinal and transverse steel had nominal yielding strengths of 540 and 650 MPa respectively. A commercially available concrete was delivered to the laboratory by a local supplier. The average concrete strength of 152 mm diameter by 305 mm high concrete cylinders at 28 days was 29.6 MPa, whereas it was 33.7 MPa during the RC beam tests. The scatter between the results of compression tests of the cylinder specimens 28 days after pouring of concrete or on the test day was negligible.

The CFRP L-shaped plates used to strengthen the RC beams were unidirectional. The L-shaped plates originally consisted of 500 mm × 200 mm legs. However, the legs of the plates had to be shortened to fit properly into the corresponding configuration of each strengthened specimen, including the embedment lengths. The L-shaped plates were 40 mm wide and 2 mm thick. The modulus of elasticity of the plates was 90 GPa according to the manufacturer’s data sheet. The ultimate tensile strength and the ultimate strain of the L-shaped plates were set to 1350 MPa and

1.3% respectively. The L-shaped plates were epoxy-bonded to the test zone in a U-shaped envelope around the web, i.e., the short legs of two L-shaped plates at one cross section overlapped onto the soffit of the specimen. The L-shaped CFRP plates were bonded to the beam surface with a two-component adhesive made of a resin and a hardener, both of which are engineered mainly for structural applications and were supplied by the manufacturer. The epoxy's mechanical properties, as specified by the manufacturer, were: 24.8 MPa bond strength, 1% elongation at break, and 4.5 GPa tensile modulus of elasticity. The CFRP sheet used for the specimens strengthened with EB FRP sheet was a unidirectional carbon-fibre fabric. It was applied continuously over the test zone in a U-shaped envelope around the web. The continuous composite material was selected because it can provide an appropriate benchmark to evaluate the effectiveness of L-shaped FRP plates in shear-strengthening of RC beams. The mechanical properties of the CFRP sheet according to the manufacturer's datasheet were as follows: 3450 MPa tensile strength, 230 GPa tensile E-modulus, 1.5% elongation at break, 1.8 g/cm^3 density, and 230 g/m^2 area weight. The CFRP fabric was bonded to the beam surface with a two-component epoxy paste made of a resin and a hardener. The mechanical properties of the epoxy paste as specified by the manufacturer were as follows: 30 MPa tensile strength, 1.5% elongation at break, and 3.8 GPa flexural modulus of elasticity. Table 2 provides the mechanical and elastic properties of the CFRP plates and sheets as provided by the manufacturers.

Test set-up and procedure

As mentioned earlier, the beams were tested in three-point load flexure. The load was applied at a distance $a = 3d$, which corresponds to a slender beam test. A carefully detailed and widely spread measuring plot was chosen for the test series. Using linear variable differential transformers (LVDTs), the vertical displacement was measured under the applied load at the mid-span. Strain gauges were carefully bonded onto the transverse- and longitudinal-steel reinforcements to measure the deformations at different loading phases. The displacement sensors, known as crack gauges, were used to measure the deformations experienced by the CFRP L-shaped plates. These gauges were installed vertically on the strengthening L-shaped plates (Fig. 2). All the tests were conducted under displacement control conditions at 2 mm/minute.

Strengthening methods

Three of the tested specimens were strengthened with epoxy-bonded L-shaped CFRP plates with different embedment lengths of the CFRP plates in the beam flange. The behaviour of the strengthened RC beams with the L-shaped CFRP plates was compared with that of the specimens strengthened with EB CFRP sheet.

To install the L-shaped CFRP plates with no embedment (S1-LS-NE), the following procedure was used: (1) the area of the specimen where the CFRP L-shaped plates were to be bonded was sand-blasted to remove the external cement paste and to round out the beam corners at the beam soffit; (2) the bond area was ground to remove any possible irregularities and to achieve a smooth bond surface; (3) residues were removed by compressed air; and (4) CFRP L-shaped plates were bonded to the bottom and lateral faces of the RC beam using a two-component epoxy resin. Note that two L-shaped plates were used in each section of the RC beam to form a U-shaped jacket. The bottom legs of the L-shaped plates were overlapped onto the soffit face of the T-beam.

In specimens S1-LS-PE and S1-LS-FE one leg of each bonded L-shaped CFRP plate was embedded in the RC beams flange to provide a form of end-anchorage to the FRP plates. To install the partially embedded L-shaped plates (S1-LS-PE), the following steps were carried out after the first three steps described above for the specimen strengthened with L-shaped plates with no embedment: (1) 25.4 mm (one-inch)-deep grooves with a cross section of 50.8 mm × 12.7 mm spaced at 175 mm were drilled perpendicular to the bottom of the beam flange at the intersection of the RC beam web and flange (Fig. 3); (2) a thin layer of epoxy paste was applied to the grooves; (3) CFRP L-shaped plates were epoxy-bonded to the web and to the soffit of the RC beam surface. Note that the extended leg of the L-shaped plate was inserted and bonded into the groove.

To bond the fully embedded CFRP L-shaped plates (S1-LS-FE) the following steps were used: (1) 102 mm (four-inch)-deep grooves with a cross section of 50.8 mm × 12.7 mm spaced at 175 mm were drilled throughout the flange thickness of the RC beam at the flange intersection with the RC beam web; (2) a thin layer of epoxy paste was applied to the grooves; (3) CFRP L-shaped plates were epoxy-bonded to the web and soffit of the RC beam surface. The extended leg of the CFRP L-shaped plate was epoxy-bonded into the groove (Fig 3).

Note that for each of the strengthening methods described above, the CFRP L-shaped plates were cut to a length that takes the embedment depth into account.

To apply the EB FRP sheet-strengthening method with no anchorage (S1-EB-NA), the following procedures were carried out: (1) the area of the specimen where the continuous CFRP sheet was to be bonded was sand-blasted to remove the exterior cement paste and to round off the beam edges; (2) the bond area was ground to remove possible irregularities and to attain a smooth bond surface; (3) residues were removed by compressed air; and (4) a U-shaped layer of continuous

CFRP sheet was glued to the soffit and lateral faces of the RC beam using a two-component epoxy resin.

RESULTS AND DISCUSSION

The experimental results obtained for all the specimens are summarized in Table 1. The results are presented in terms of the loads attained at failure; the experimental shear resistance due to concrete, transverse steel, and CFRP; and the shear-capacity gain due to CFRP. Note that the shear contributions of concrete (V_c) and steel (V_s) were calculated based on the results achieved from the control test specimens, i.e., S0-CON and S1-CON. Some of the values provided in Table 1 are calculated based on the following assumptions, which are implicitly stated in the design guidelines: a) the shear resistance due to concrete is the same whether or not the beam is reinforced with transverse steel and whether or not the beam is strengthened with CFRP; and b) the shear resistance due to steel is the same whether or not the beam is strengthened with CFRP.

The results reveal that the shear-capacity gain due to CFRP for the specimen strengthened with fully embedded L-shaped plates was 55%, compared to 39%, 36%, and 27% respectively for the corresponding specimens strengthened with partially embedded L-shaped plates, EB sheets, and L-shaped plates with no embedment.

These results clearly confirm the effectiveness of all the strengthening methods used in this research study, especially the method of shear-strengthening RC beams with L-shaped CFRP plates with full or partial embedment (specimens S1-LS-FE and S1-LS-PE).

Table 1 reveals that the beams strengthened using fully embedded CFRP L-shaped plates (S1-LS-FE) and partially embedded CFRP L-shaped plates (S1-LS-PE) attained the highest shear resistance due to FRP strengthening, compared to the other two strengthened specimens (S1-LS-

NE and S1-EB-NA). Specimens S1-LS-FE and S1-LS-PE respectively reached 119.5 kN and 84.1 kN shear resistance due to FRP. Specimens S1-LS-NE and S1-EB-NA respectively reached 59.2 kN and 77.8 kN shear resistance due to FRP.

Failure progression

All the test specimens failed in shear except for the S1-LS-FE specimens. It should be emphasized that for the specimens with transverse steel, shear failure occurred after the transverse steel intersecting with the shear crack had yielded. Failure of each specimen can be described as follows:

S0-CON: The unstrengthened specimen with no transverse-steel reinforcement failed due to diagonal tension failure in a brittle manner. A diagonal shear crack formed during the loading of beam S0-CON at a load of 78.8 kN. As the load increased, the crack widened and propagated until failure, which occurred at a load of 122.7 kN.

S1-CON: The control beam with transverse-steel reinforcement spaced at 175 mm (s=d/2) developed diagonal shear cracks at a load similar to that at which the shear crack started propagation in S0-CON (78.2 kN). Specimen S1-CON failed due to diagonal tension failure at a load of 432.4 kN, followed by the rupture of the second stirrup located at 263 mm from the support.

S1-LS-NE: Beam S1-LS-NE had the same transverse-steel reinforcement as the control specimen S1-CON, but was strengthened with epoxy-bonded CFRP L-shaped plates without any embedment of the L-shaped plates in the RC beam flange. The ultimate load attained was 550.7 kN, that is, 27% greater than the ultimate capacity of S1-CON. Specimen S1-LS-NE failed due to debonding of the FRP plates followed by diagonal tension failure of the beam (Fig. 4). Note that the longitudinal-steel reinforcement yielded before the ultimate shear failure.

S1-LS-PE: The ultimate load was attained at 600.5 kN, that is, 39% greater than the ultimate capacity of the S1-CON control beam and 9% greater than the ultimate capacity of S1-LS-NE. Specimen S1-LS-PE failed due to break-out of the FRP plate from the concrete flange around the embedded L-shaped FRP plate, which was followed by debonding of the FRP plate from the RC beam web (Fig. 5). Similarly to specimen S1-LS-NE, the longitudinal-steel reinforcement yielded before the ultimate shear failure.

S1-LS-FE: The ultimate load attained was 671.4 kN, which was 55% greater than the shear capacity of control beam S1-CON and 22% greater than the ultimate shear capacity of S1-LS-NE. No sign of CFRP plate debonding was observed. Failure occurred by yielding of longitudinal steel followed by flexural compression failure (Fig. 6).

S1-EB-NA: Beam S1-EB-NA had similar transverse-steel reinforcement to the control specimen S1-CON, but was strengthened with epoxy-bonded CFRP sheet with no anchorage. The ultimate load attained 587.9 kN, that is, 36% greater than the ultimate capacity of S1-CON and 7% greater than the ultimate capacity of S1-LS-NE. Specimen S1-EB-NA failed due to debonding of the CFRP sheet followed by diagonal tension failure (Fig. 7). The longitudinal-steel reinforcement yielded before the ultimate shear failure.

Deflection response

Figure 8 presents load versus maximum deflection curves at the mid-span for beams strengthened with FRP L-shaped plates and sheets and for the control beams. The maximum load at failure and the maximum deflection attained at the loading point for each specimen are provided in Table 1. Specimen S1-LS-FE exhibited a higher deflection at the loading point than the other strengthened and unstrengthened specimens. Moreover, specimen S1-LS-FE achieved a higher maximum load at failure than the rest of the specimens (Table 1). Specimen S1-LS-FE was the only one that reached its flexural capacity limit (Fig. 8). Therefore, the failure of specimen S1-LS-FE was more ductile compared to other strengthened and unstrengthened specimens. Note that specimens S1-LS-NE, S1-LS-PE, and S1-EB-NA also failed in a ductile manner. The longitudinal steel in specimens S1-LS-NE, S1-LS-PE, and S1-EB-NA yielded before the ultimate shear failure. Nevertheless, specimen S1-LS-FE reached the maximum displacement ductility factor (μ) among all the strengthened beams. The maximum displacement ductility factor of S1-LS-FE was 5.64, whereas μ was 1.70, 2.69, and 2.37 for S1-LS-NE, S1-LS-PE, and S1-EB-NA respectively. The deflection ductility is defined here as the ratio of the maximum attained deflection to the displacement corresponding to yielding. It can be seen that the deflection behavior of the beams strengthened with fully embedded and partially embedded L-shaped CFRP plates is more ductile than that of the other effective shear-strengthened specimens (Table 1). For example, the deflection under point load of beam S1-LS-FE at maximum load was 2.17 times that of beam S1-LS-NE at maximum load (42.9 mm at load 671.4 kN versus 19.8 mm at 550.7 kN) and 2.01 times that of beam S1-EB-NA at maximum load (42.9 mm at load 671.4 kN versus 21.3 mm at 587.9 kN), whereas the S1-CON beam failed at a maximum load of 432.4 kN with a maximum deflection at the mid-span of 11.9 mm.

Strain in transverse steel

Curves representing applied load versus strain in the transverse-steel reinforcement are presented in Fig. 9. It is clear that the transverse-steel reinforcement contributed very little to the load-carrying capacity in the early stages of loading. The transverse steel started to contribute to shear resistance only after shear diagonal cracks formed in the concrete. The transverse-steel contribution was initiated at applied loads of between 50 and 100 kN for all the test specimens. The transverse-steel strain continued to increase sharply as the applied load increased until either the transverse steel yielded at 3250 μstrains or ultimate failure of the specimen occurred. Figure 9 shows that the transverse steel crossing the shear crack lines yielded in all the specimens tested in this study.

Given the applied load, the strain in the transverse steel was relatively less in specimens S1-LS-PE, S1-LS-FE, and S1-EB-NA than in specimens S1-CON and S1-LS-NE (Fig. 9). This could be due to the effectiveness of FRP in specimens S1-LS-PE, S1-LS-FE, and S1-EB-NA compared to specimens S1-CON and S1-LS-NE (Table 1). Figure 9 reveals that for the specimens with greater shear-capacity gain due to CFRP, the transverse steel experienced less strain during the tests. Therefore, it can be concluded that the CFRP strengthening method effectively eased the strains in the transverse steel. Hence, the transverse steel yielded at a greater applied load in specimens that were effectively strengthened with FRP compared to the corresponding specimens with no FRP strengthening or with less effective FRP strengthening methods. The reported transverse-steel strain is the measured strain in the steel stirrup that reached the maximum strain during loading.

Strain in FRP

In this part of the study, the CFRP strain readings for all the strengthened specimens were analyzed. Figure 10 shows the load versus FRP strain curves for the beams strengthened with L-shaped FRP plates and EB U-jacket sheets. The curves show that for the strengthened specimens (except for S1-LS-PE and S1-LS-FE), the CFRP did not contribute to load-carrying capacity in the initial stage of loading until the applied load reached between 180 and 200 kN. In specimens S1-LS-PE and S1-LS-FE, the FRP started to contribute to shear resistance at a loading of 50 kN. This could be due to the embedment of the L-shaped FRP plates into the concrete flange, which might have rendered the L-shaped CFRP plates effective at an earlier stage of loading than in specimens S1-LS-NE and S1-EB-NA.

In all specimens, after the CFRP started to contribute to shear resistance, the CFRP strain continued to increase sharply under increasing load. The increase in the FRP strain continued to a certain limit that differed from one specimen to another, depending on the strengthening method, before the strain started to increase drastically. The maximum strain recorded corresponding to the mentioned limit reached 4262 $\mu\varepsilon$, 2085 $\mu\varepsilon$, 3061 $\mu\varepsilon$, and 1080 $\mu\varepsilon$ for specimens S1-LS-NE, S1-LS-PE, S1-LS-FE, and S1-EB-NA respectively. Ultimately, the CFRP strain rate started to increase drastically as the load increased further. This could be due to yielding of transverse steel, which further engaged the CFRP to contribute more to the shear resistance of the RC beams. The rapid increase in CFRP strain continued until ultimate failure took place.

Figure 10 shows that the FRP strain in specimens strengthened with partially and fully embedded L-shaped CFRP plates was distributed more effectively than in specimens strengthened with L-shaped FRP and EB sheets with no anchorage. Unlike specimens S1-LS-NE and S1-EB-NA, specimens S1-LS-PE and S1-LS-FE had the following positive features: (i) the FRP contributed to the shear resistance in the early stages of loading (it was effective at service loads); (ii) the FRP strain increased almost linearly with applied load; (iii) no drastic decrease in FRP strain was observed at ultimate failure, or in other words, FRP debonding was avoided. Note that the reported strain values were not necessarily the absolute maximum values experienced by the CFRP, but the maximum measured values. The two values could be different if the strain gauges did not intercept the main cracks.

Strain in longitudinal-steel reinforcement

Figure 11 presents the variation with applied load of the strains in the longitudinal-steel reinforcement. These curves show that most of the curves for load versus strain in longitudinal steel coincide (except for specimen S1-EB-NA). The flexural stiffness of specimen S1-EB-NA, which was strengthened with continuous CFRP sheets, was slightly greater than that of both the control beam and the beams strengthened with CFRP L-shaped plates (Fig. 11). The greater flexural stiffness in specimen S1-EB-NA could be due to the effect of CFRP sheet continuity. The uniaxial CFRP sheet used in this study could also carry some load in the direction perpendicular to its fibre orientation because the sheet has a tensile modulus of 5876 MPa and a tensile strength of 27 MPa in the minor direction (90°).

Overall, the longitudinal-steel reinforcement reached yielding between applied loads of 471 to 516 kN in all the strengthened specimens. However, the ultimate failure of specimens S1-LS-PE, S1-LS-NE, and S1-EB-NA occurred due to diagonal tension failure of the concrete cross section.

Efficiency of L-shaped CFRP plates versus CFRP sheets

Table 1 shows that the specimen strengthened with fully embedded CFRP L-shaped plate experienced significant increase in shear capacity with respect to the control beams and other strengthened specimens. Specimen S1-LS-FE failed at a loading of 671.4 kN in flexural compression failure mode, whereas specimens S1-LS-PE, S1-LS-NE, and S1-EB-NA failed in shear at loadings of 600.5 kN, 550.7 kN, and 587.9 kN respectively. The shear contribution of FRP for specimens S1-LS-FE, S1-LS-PE, S1-LS-NE, and S1-EB-NA was 119.5 kN, 84.1 kN, 59.2 kN, and 77.8 kN respectively. However, it is important to quantify the efficiency of the FRP shear-strengthening methods in terms of the shear contribution of FRP versus the amount of FRP used.

To define the efficiency of CFRP for each of the strengthening methods used in this study, the amount of FRP per unit length was calculated. The cross-sectional area of CFRP bonded to both sides of the web per metre of shear span used in all specimens strengthened with L-shaped CFRP plates (with or without embedment of the plate) was 914 mm^2/m. For the specimens strengthened with EB FRP sheets, the cross-sectional area of CFRP per metre of shear span was 254 mm^2/m. The ultimate tensile capacity per unit length of the retrofitted specimens with L-shaped CFRP plates (with or without plate embedment) was 1234 kN/m. For the specimens strengthened with EB FRP sheets, the ultimate tensile capacity per unit length was 882 kN/m.

The efficiency of CFRP (Ψ_f) is a tool that enables researchers to quantify rationally and hence to compare the effectiveness of various strengthening methods involving application of FRP material. The efficiency of a FRP strengthening method (Ψ_f) for an RC beam is defined as the shear contribution of FRP, V_f, divided by the ultimate tensile capacity per unit length of the FRP used in the strengthened beam. Table 3 shows the efficiency of each of the FRP strengthening methods used in this study. It can be seen that the beam strengthened with fully embedded CFRP L-shaped plates reaches the highest FRP efficiency among all the strengthened beams in this study. Note that in this comparison, the dry fibre material characteristics of the CFRP sheet are based on manufacturers' data sheets.

CONCLUSIONS

Prefabricated L-shaped CFRP plates can enhance significantly the shear capacity of RC beams. In this study, the average increase in shear capacity reached 40% for the beam retrofitted with epoxy-bonded L-shaped CFRP plates. Within the experimental scope of this research study, the following conclusions can be drawn:

- The effective application of partially embedded L-shaped CFRP plates to shear-strengthening of RC beams was verified based on experimental investigations.
- Among the tested specimens, partial embedment of L-shaped CFRP plates was the most effective alternative to full embedment of L-shaped CFRP plates when full embedment of L-shaped plates is not feasible.
- Specimens strengthened with partially and fully embedded L-shaped FRP plates (S1-LS-PE and S1-LS-FE) reached the highest gain in shear resistance due to FRP strengthening and outperformed the other strengthened specimens with no embedment or anchorage (S1-LS-NE and S1-LS-NA).
- In specimen S1-LS-FE, shear failure was prevented by effective embedment of the plate in the concrete beam flange. Specimen S1-LS-FE failed in a ductile manner in flexure with a maximum displacement ductility factor of 5.64.
- Unlike specimens S1-LS-NE and S1-EB-NA, specimens S1-LS-PE and S1-LS-FE had the following positive features: (i) the FRP contributed to shear resistance at early stages of loading (it was effective at service loads); (ii) the strain in the FRP increased almost linearly with applied load; and (iii) no drastic decrease in FRP strain was observed at ultimate failure, or in other words, FRP debonding was avoided.

ACKNOWLEDGMENTS

The authors wish to acknowledge the support provided by the Natural Sciences and Engineering Research Council of Canada through a postdoctoral fellowship to Dr. Mofidi and to Prof. Chaallal through a Discovery grant. The authors thank Sika Canada Inc. (Pointe Claire, Quebec) for providing the epoxy and the CFRP L-shaped plates. The efficient collaboration of John Lescelleur (senior technician) and Juan Mauricio Rios (technician) is acknowledged.

REFERENCES

Chaallal, O., Nollet, M.J., and Perraton, D. (1998). Strengthening of reinforced concrete beams with externally bonded fibre-reinforced plastic plates: design guidelines for shear and flexure. *Can. J. Civil Eng.* 25(4), 692–704.

Chen, J. and Robertson, I. (2004). Test of cracked pre-stressed concrete T-beam retrofitted for shear using CFRP L-shaped plates. *University of Hawaii Research Report UHM/CEE/04-06.*

Chen, J.F. and Teng, J.G. (2003). Shear capacity of FRP-strengthened RC beams: FRP debonding. *Construction and Building Materials* 17(1), 27–41.

Czaderski, C. (1998). Nachträgliche schubverstärkung mit CFK-Winkeln. *Schweizer Ingenieur und Architekt (SI + A)* 43(22). 822–826 (in German).

Czaderski, C. and Motavalli, M. (2004). Fatigue behaviour of CFRP L-shaped plates for shear strengthening of RC T-beams. *Composites: Part B* 35, 279–290.

De Lorenzis, L. (2004). Anchorage length of near-surface-mounted fibre-reinforced polymer rods for concrete strengthening: analytical modeling. *ACI Struct. J.* 101(3), 375–386.

De Lorenzis, L. and Nanni, A. (2001). Shear strengthening of reinforced concrete beams with NSM fibre-reinforced polymer rods. *ACI Struct. J.* 98(1), 60–68.

EMPA Test Report 116/7 (2002). Shear strengthening with prefabricated CFRP L-shaped plates: test beams S1 to S6. *Eidgenössische Materialprüfungs- und Forschungsanstalt*, 79 pages.

Khalifa, A., Gold, W.J., Nanni, A., and Aziz, A. (1998). Contribution of externally bonded FRP to shear capacity of RC flexural members. *J. Compos. Constr.* 2(4), 195–203.

Meier, H., (1998). CFK-Schubverstärkungselemente. *Schweizer Ingenieur und Architekt (SI + A)* 43(22), 819–821 (in German).

Mofidi, A. and Chaallal, O. (2011a). Shear strengthening of RC beams with epoxy-bonded FRP—influencing factors and conceptual debonding model. *Journal of Composites for Construction* 15(1), 62–74.

Mofidi, A. and Chaallal, O. (2011b). Shear strengthening of RC beams with externally bonded FRP composites: effect of strip-width to strip-spacing ratio. *Journal of Composites for Construction* 15(5), 732–742.

Mofidi, A., Chaallal, O., Benmokrane, B., and Neale, K.W. (2012a). Performance of end-anchorage systems for RC beams strengthened in shear with epoxy-bonded FRP. *Journal of Composites for Construction* 16(3), 322–331.

Mofidi, A., Chaallal, O., Benmokrane, B., and Neale, K.W. (2012b). Experimental tests and design model for RC beams strengthened in shear using the embedded through-section FRP method. *Journal of Composites for Construction* 16(5), 540–550.

Mofidi, A., Thivierge, S., Chaallal, O., and Shao, Y. (2013). Behavior of reinforced concrete beams strengthened in shear using L-shaped CFRP plates. II: Design modeling. *Journal of Composites for Construction*, in press.

Monti, G. and Liotta, M. (2006). Tests and design equations for FRP strengthening in shear. *Construction and Building Materials* 21, 799–809.

Robertson, I., Johnson, G.P., and Sharma, B. (2007). Shear retrofit of concrete T-beams using CFRP. *Proc. 8rd Int. Symp. on Fibre-Reinforced Polymers in Reinforced Concrete Structures*, Patras, Greece.

Triantafillou, T.C. (1998). Shear-strengthening of reinforced concrete beams using epoxy-bonded FRP composites. *ACI Struct. J.* 95(2), 107–115.

Uji, K. (1992). Improving shear capacity of existing reinforced concrete members by applying carbon fibre sheets. *Trans. Jpn. Concr. Institute* 14, 253–266.

Table 1 – Experimental results.

Specimen	Load at rupture	Total shear resistance	Resistance due to concrete	Resistance due to steel	Resistance due to CFRP	Gain due to CFRP	Deflection at load point	Failure mode
	kN	kN	kN	kN	kN	%	mm	
S0-CON	162.4	81.2	81.2	0.0	0.0	0	2.6	Shear
S1-CON	432.4	216.2	81.2	135.0	0.0	0	11.9	Shear
S1-LS-NE	550.7	275.4	81.2	135.0	59.2	27	19.8	Shear
S1-LS-PE	600.5	300.3	81.2	135.0	84.1	39	19.2	Shear
S1-LS-FE	671.4	335.7	81.2	135.0	119.5	55	42.9	Flexure
S1-EB-NA	587.9	294.0	81.2	135.0	77.8	36	21.3	Shear

Table 2 – Mechanical properties of CFRP L-shaped plate and CFRP sheets used.

Property	L-shaped CFRP plate	Dry fibre sheet	Wet layup FRP sheet
Modulus of elasticity, GPa	90	230	65
Ultimate elongation, %	1.30	1.50	1.33
Ultimate stress, MPa	1350	3450	894

Table 3 – Efficiency of FRP using different strengthening methods.

Specimen	Area of CFRP	Ultimate tensile capacity per unit length	V_f	ψ_f Efficiency of FRP
	mm^2/m	kN/m	kN	%
S1-LS-NE	914	1234	59.2	4.8
S1-LS-PE	914	1234	84.1	6.8
S1-LS-FE	914	1234	119.5	9.7
S1-EB-NA	256	882	77.8	8.8

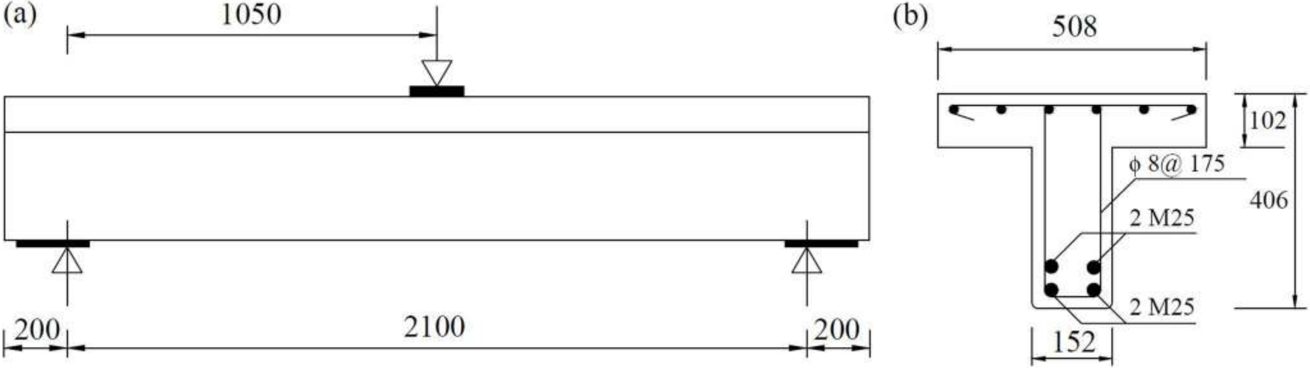
(a)
1050
200
2100
200
(b)
508
102
406
ϕ 8@ 175
2 M25
2 M25
152


100

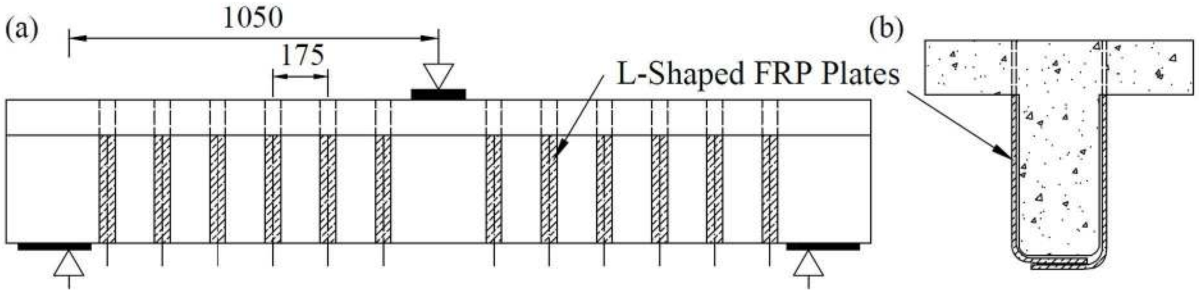
(a)
1050
175
L-Shaped FRP Plates
(b)


LS-4L
LS-4R

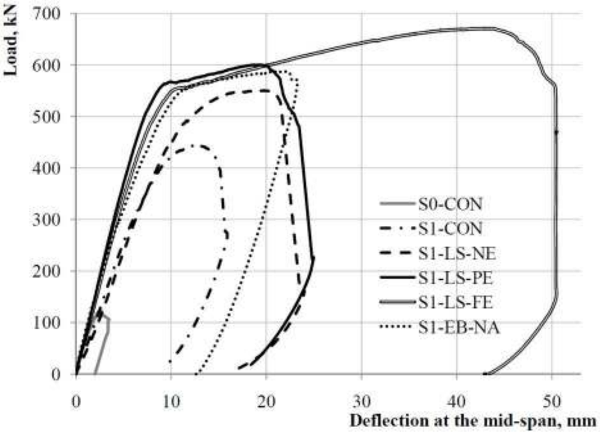

Load, kN
700
600
500
400
300
200
100
0
0
10
20
30
40
50
Deflection at the mid-span, mm
S0-CON
S1-CON
S1-LS-NE
S1-LS-PE
S1-LS-FE
S1-EB-NA

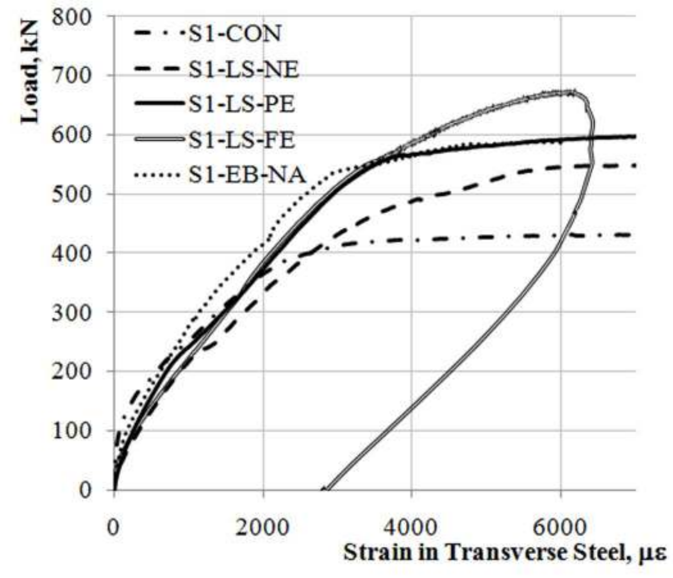

Load, kN
800
700
600
500
400
300
200
100
0
S1-CON
S1-LS-NE
S1-LS-PE
S1-LS-FE
S1-EB-NA
0
2000
4000
6000
Strain in Transverse Steel, με

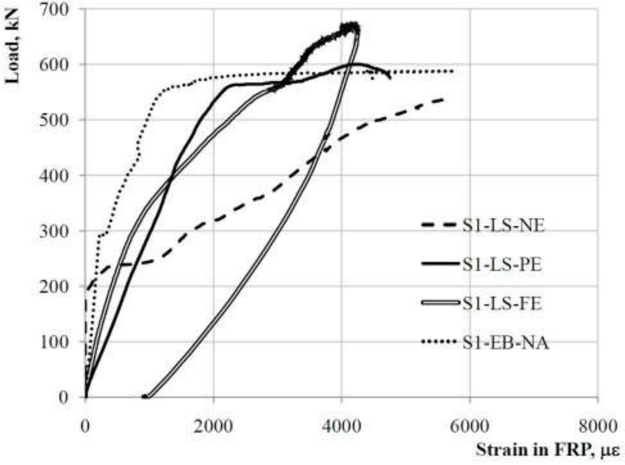
Load, kN
700
600
500
400
300
200
100
0
0
2000
4000
6000
8000
Strain in FRP, με
S1-LS-NE
S1-LS-PE
S1-LS-FE
S1-EB-NA

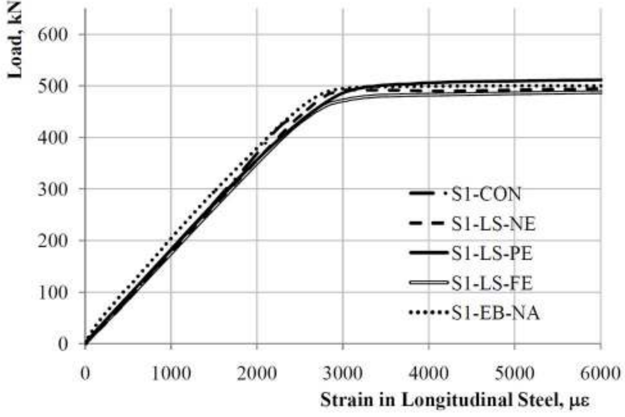
Load, kN
600
500
400
300
200
100
0
0
1000
2000
3000
4000
5000
6000
Strain in Longitudinal Steel, με
S1-CON
S1-LS-NE
S1-LS-PE
S1-LS-FE
S1-EB-NA